Integration of On-chip Isotachophoresis and Functionalized Hydrogels for Enhanced-Sensitivity Nucleic Acid Detection

Giancarlo Garcia-Schwarz and Juan G. Santiago*

Department of Mechanical Engineering, Stanford University, Stanford, CA 94305, USA

*E-mail: juan.santiago@stanford.edu

Supporting Information

S1. Reagents and Materials

We purchased trizma base, 4-(2-Hydroxyethyl)piperazine-1-ethanesulfonic (HEPES), 3-(trimethoxysilyl)-propyl methacrylate, 40% acrylamide/bisacrylamide (29:1), and 70% perchloric acid from Sigma-Aldrich (St. Louis, MO). We purchased the photoinitiator 2,2-azobis[2-methyl-N-(2-hydroxyethyl) propionamide] (VA-086) from Wako Chemicals (Richmond, VA). We also purchased hydrochloric acid from J.T. Baker (Avantor Performance Materials, Center Valley, PA); and Tris-EDTA buffer, magnesium chloride, and 30% hydrogen peroxide from EMD biosciences (Gibbstown, NJ). We purchased glacial acetic acid and sodium hydroxide from Mallinckrodt Chemicals (Avantor Performance Materials, Center Valley, PA). The DNase/RNase-Free distilled water and pre-mixed 1M Tris-HCl pH 8 was purchased from GIBCO (Carlsbad, CA). We purchased formamide from Invitrogen (Carlsbad, CA). We purchased the synthetic DNA and RNA oligonucleotides listed in **Table S1** from Genelink (Hawthorne, NY) and Integrated DNA Technologies (Coralville, IA). We stored reconstituted oligos in either Tris-EDTA buffer (let-7a precursor) or 10 mM Tris-HCl (all others), and stored these oligo stock solutions at either -20°C or -80°C in 5–20 µl aliquots.

We purchased crown glass microfluidic chips (model NS260) and separate plastic chip caddies from Caliper Life Sciences (Mountain View, CA). We attached chip caddies using ultra-violet (UV)-curing optical adhesive (NOA-68) purchased from Norland Products Inc. (Cranbury, NJ) and a UV lamp purchased from Zilla Products (Franklin, WI).

We performed UV-initiated polymerization of polyacrylamide hydrogels by filling chips with prepolymer solution, as described in **Section S4**, and placing chips atop a 365 nm collimated LED lightsource (M365L2-C3) from Thorlabs (M365L2, Newton, NJ). We measured UV lightsource intensity (approximately 5 mW/cm^2 at the chip plane) using a digital UV light meter (UV513AB, General Tools, New York, NY).

S2. Experimental apparatus

All data were taken with a custom epifluorescent point-confocal microscopy setup described by Bercovici *et al.*[1,2] **Fig. S1** shows a schematic of the experimental setup. Briefly, the setup consists of an inverted epifluorescent microscope (IX70, Olympus, Hauppauge, NY) with 60x water-immersion objective (LUMPlanFL, Olympus, Hauppauge, NY) and Cy5 filter cube (Cy5-

4040A, Semrock, Rochester, NY). The microscope was outfitted with an XYZ automated stage (ASI, Eugene, OR). A 642 nm diode laser (Stradus-642, Vortran Laser Technologies, Sacramento, CA) was used for illumination and a photomultiplier tube (PMT) module (H6780-20, Hamamatsu Photonics, Japan) with data acquisition unit (C8908, Hamamatsu Photonics, Japan) for detection. The PMT was powered by a function generator (E3631A, Agilent Technologies, Santa Clara, CA) and operated at a rate of 66.7 Hz (15 ms sampling period with 10 ms integration time). We used a high-voltage sourcemeter (2410, Keithley Instruments, Cleveland, OH) to apply constant current to the microfluidic chip. We used a custom MATLAB (R2007b, Mathworks, Natick, MA) program to control the high voltage supply and PMT and to record data from both instruments.

S3. Preparation of prepolymer mastermix, ITP buffers, and surface modification reagents

Composition of our prepolymer is similar to that used by He *et al*.[3] We prepared a prepolymer mastermix in order to minimize variation in composition. We prepared this mastermix by combining 1 M HCl (5.11 g), 1 M tris (10.3 g), 40% acrylamide/bisacrylamide (5.04 g), water (26.2 g), and magnesium chloride (500 µl). We prepared the photoinitiator, VA-086, daily at a concentration of 2% (w/v). Using these components and acrydite-modified oligos we prepared (daily) three distinct leading electrolyte (LE) prepolymer mixtures:

LE0: 187 µl mastermix + 13 µl VA-086

LE1: 69 µl LE0 + 1 µl acr-loop-pre7a

LE2: 19 µl LE0 + 1 µl acr-7a

We found that fresh preparation of the photoinitiator VA-086 before each use was important, as this reagent is unstable under exposure to light and in aqueous solution.[3] The TE consisted of 10 mM HEPES, 20 mM Tris, and 90% formamide. Before each experiment, we combined 90 µl TE, 7 µl water, and 1–2 µl target microRNA. We then heated this mixture in a water bath at 60°C for 5 min to disrupt secondary structure and then immediately placed on ice. Finally, we added 2 µl of 100 nM rep-7a to this mixture (for a final volume of 100 µl) before using in the experiment. We refer to this mixture as TE+S in the following sections and figures.

We prepared a surface modification mixture and used it to modify channel surface properties and promote covalent attachment of hydrogel to the glass surface (see **Section S4** for details). This mixture consisted of 5:3:2 (v/v) DI water, acetic acid, and 3-(trimethoxysilyl)-propyl methacrylate.

S4. Chip Preparation and Patterning of Functionalized Polyacrylamide Gels

To create mechanically-stable hydrogels within the microfluidic channels, we used the surface-modifier 3-(trimethoxysilyl)-propyl methacrylate to covalently attach the polyacrylamide gel to the glass channel surface. This method has been applied with great success by the groups of Fréchet, Svec, and coworkers[4] and Singh, Hatch, and coworkers.[5,6] For our work, we adapted the

protocol reported by Hatch *et al.*[5] We refer to channel "rinsing" as filling all reservoirs and applying vacuum at reservoirs 3 and 7 using a single split vacuum line (see **Fig. S2** for chip layout). Our protocol can be described as follows:

1. Rinse with 1 M sodium hydroxide for 10-20 min
2. Rinse with DI water for 1 min
3. Empty reservoirs and apply vacuum to dry for 1 min
4. Rinse with surface modification mixture for 5 min
5. Rinse with 30% acetic acid for 1 min
6. Rinse with DI water 1 min
7. Empty reservoirs and apply vacuum to dry for 1 min

Following this surface coating procedure, we filled the chip with prepolymer solution. **Fig. S2** shows the chip layout. We filled reservoirs 1 through 6 with 10 µl LE0 (for the limit of detection experiments, **Fig. 2**) or LE1 (for the precursor experiments, **Fig. 3**) each and reservoirs 7 and 8 with 10 µl LE2 each. We then applied vacuum to the microfluidic chip (at reservoirs 3 and 7) for approximately 1.5 min. We then carefully removed both vacuum lines simultaneously and quickly transferred the chip to our UV LED light source. Finally, we then exposed the entire chip with UV light (with ~5 mW/cm^2 intensity) for 10 min.

Following UV exposure, we flushed away unattached oligos from the channel by applying 3 µA current between reservoirs 8 and 1 for 5 min. For the precursor removal experiments (c.f., **Fig. 3** in the main manuscript), we first replaced the contents of reservoirs 1 and 6 with buffer consisting of 100 mM HCl, 200 mM Tris, and 2.5 mM $MgCl_2$, and then applied 3 µA current between reservoirs 8 and 1 for 5 min and between reservoirs 8 and 6 for 1 min to flush away unattached oligos.

S5. Estimate of gel capacity

During polymerization, we used a DNA concentration in the capture region of 25 µM. However, due inefficiencies in incorporation of acrydite-labeled oligos into the hydrogel matrix, we expect the concentration of immobilized oligos to be somewhat less than this. For example, Chan & Krull found ~45% probe incorporation efficiency in 12.5%T polyacrylamide gels.[7] Rubina *et al*. found ~83% probe incorporation efficiency in 20%T polyacrylamide gels.[8] As a rough approximation, we here estimate our incorporation efficiency by using these published values and assuming it scales directly with monomer concentration. For our 4%T polyacrylamide gels, we then estimate the immobilized capture probe concentration is approximately 4 µM. By comparison, we estimate the concentration of reporters in the ITP zone is on the order of 1 to 10 µM. The ITP zone has an approximate length of 10 µm along the channel axis, while the capture region is approximately 1 cm long. Therefore, we estimate that the capture gel has approximately 1000 times the capacity needed to remove all of the focused reporter molecules.

S6. Assay operation and data analysis

We performed our assay immediately following chip preparation, as described in the previous section. In future work, we hope to explore methods of preparing and storing our hydrogel devices. Our assay operation consisted of two stages: sample injection and signal detection. In the first stage, we injected target molecules and reporters continuously through a semi-infinite injection. In the second stage, we switched the source of TE anions to a secondary TE reservoir containing only TE (without target or reporter molecules). We used this two-stage, "finite injection" strategy in order to eliminate increase in background signal during the capture phase of the experiment. We found that this injection mode provided larger enhancement ratios and therefore improved sensitivity and dynamic range (compared to a semi-infinite injection scheme where we continuously draw target from the same TE reservoir).

We first cleaned the contents of reservoirs 1 and 6 by filling repeatedly with water and then replaced their contents with TE+S and TE, respectively. We then carried out the sample injection and detection sourcemeter protocols summarized in **Table S2**. Sample injection ended when the ITP zone reached detection station 1 (DS1), as shown in the chip schematic of **Fig. S2**. Sample injection lasted ~410 s. For sample injection we set the laser to 1 mW power output. We then switched the ground electrode to reservoir 6 and performed the detection portion of the protocol, which lasted ~190 s and ended with detection of the focused hybridized reporters at DS2 (see **Fig. S2**). For sample detection we set the laser to 1 or 4 mW power output.

Data analysis consisted of fitting a Gaussian to both injection and detection peaks, then integrating these fitted Gaussian curves to quantify signal intensity. The repeatability of the injection signal is demonstrated in **Fig. S3**, where we plot the integral of the fitted Gaussian for multiple injections corresponding to limit of detection experiments (including negative controls, 2.8 pM and 140 pM let-7a concentrations, and 140 pM miR-15a concentration). The standard deviation is 10.2% of the mean. We attribute this variation to chip-to-chip variability as well as variability in the polymerization process. In analyzing our data, we used the DS1 integral value as an internal control. The key signal in our assay is the integrated signal peak at DS2 (downstream of the start of the capture gel) normalized by the integrated signal peak at DS1. This normalization helps normalize against chip-to-chip and experiment-to-experiment variations in the ITP pre-focusing and mixing processes. **Fig. S4** shows typical signals and Gaussian fits for titration experiment data (used for **Fig. 2B**).

S7. Protocol for gel dissolution and chip regeneration

We adapted our chip regeneration protocol from that used by He *et al*.[3] Immediately following completion of an experiment (with chip reservoirs still filled with liquid), we removed the microfluidic chip from its plastic caddy by carefully bending the caddy to result in adhesive delamination. We then stored the chip in water (indefinitely) or immediately transferred to a gel dissolution bath. The gel dissolution bath consisted of a 2:1 (v/v) mixture of perchloric acid and hydrogen peroxide heated to ~70°C on a hotplate. Chips were left to soak in this bath at least overnight before ready for reuse.

S8. Numerical Simulation of ITP-enhanced Hybridization Reaction

We model ITP-enhanced hybridization with a three-species bulk reaction model. Each species is represented by a bulk concentration, c_i, where the index i stands for target (T), reporter (R), or hybrid (H) molecules. In experiments, target and reporter molecules were initially mixed together in the TE reservoir and focused in the ITP zone continuously through a semi-infinite injection.[9] After 410 s, we switched ground voltage to a "clean" TE reservoir containing solution with no target or reporter molecules for approximately 190 s. The rate of change of species concentrations therefore depends on both hybridization kinetics as well as ITP focusing rate of reaction species as follows:

$$\frac{dc_H}{dt} = k_{on}c_R c_T - k_{off}c_H$$
$$\frac{dc_T}{dt} = -k_{on}c_R c_T + k_{off}c_H + Fc_{T,0}$$
$$\frac{dc_R}{dt} = -k_{on}c_R c_T + k_{off}c_H + Fc_{R,0}$$

Here t is time and k_{on} and k_{off} are the kinetic on- and off-rates, respectively. The concentrations of target and reporter molecules in the TE are $c_{T,0}$ and $c_{R,0}$, respectively. The species concentrations c_H, c_T, and c_R may be interpreted as concentrations of hybrid, target, and reporter molecules volume-averaged over the ITP zone. For all numerical simulations, we take $k_{on} = 10^6$ M^{-1} s^{-1} and $k_{off} = 10^{-15}$ s^{-1}. These values are in agreement with existing on-rate measurements for short (~23 nt) oligos[10] and equilibrium constants calculated using the DINAMelt web server.[11] We solved these coupled ordinary differential equations using MATLAB's ode45. The single fitting parameter, F, represents the flux (per concentration) of molecules (with units of s^{-1}) from the TE into the focused sample zone during the injection period. We find that taking $F = 0.0024$ s^{-1} results in the best model fit to titration curve data shown in **Fig. 2B**.

Our numerical model determines the fraction of hybridized reporters over time given an influx rate (F) of target and reporter molecules. This process is depicted in **Fig. S5**, where we plot the fraction of hybridized reporters over time for a range of initial target concentrations. The vertical dashed lines represent the end of the injection cycle (at 410 s) and detection (at 600 s) portions of the voltage control program. At the end of the injection portion, we set $F = 0$ (no influx of target and reporter molecules into the ITP zone) in the unsteady simulation.

References

(1) Bercovici, M.; Kaigala, G. V.; Mach, K. E.; Han, C. M.; Liao, J. C.; Santiago, J. G. *Anal. Chem.* **2011,** 83, 4110-4117.

(2) Bercovici, M.; Han, C. M.; Liao, J. C.; Santiago, J. G. *Proc. Natl. Acad. Sci. U.S.A.* **2012**, DOI:10.1073/pnas.1205004109.

(3) He, M.; Herr, A. E. *Nat. Protoc.* **2010,** 5, 1844-1856.

(4) Rohr, T.; Yu, C.; Davey, M. H.; Svec, F.; Fréchet, J. M. *Electrophoresis* **2001,** 22, 3959-3967.
(5) Hatch, A. V.; Herr, A. E.; Throckmorton, D. J.; Brennan, J. S.; Singh, A. K. *Anal. Chem.* **2006,** 78, 4976-4984.
(6) Sommer, G. J.; Singh, A. K.; Hatch, A. V. *Lab Chip* **2009,** 9, 2729-2737.
(7) Chan, A.; Krull, U. J. *Anal. Chim. Acta* **2006**, 578, 31-42
(8) Rubina, A. Y.; Pan'kov, S. V.; Dementieva, E. I.: Pen'kov, D. N.; Butygin, A. V.; Vasiliskov, V. A.; Chudinov, A. V.; Mikheikin, A. L.; Mikhailovich, V. M.;Mirzabekov, A. D. *Anal. Biochem.* **2004**, 325, 92-106.
(9) Khurana, T. K.; Santiago, J. G. *Anal. Chem.* **2008,** 80, 6300-6307.
(10) Gao, Y.; Wolf, L. K.; Georgiadis, R. M. *Nucleic Acids Res* **2006,** 34, 3370-3377.
(11) Markham, N. R.; Zuker, M. *Nucleic Acids Res* **2005,** 33, W577-W581.

Table S1. Synthetic oligonucleotide sequences with associated purification methods and purity estimates. Purification methods included high pressure liquid chromatography (HPLC) and polyacrylamide gel electrophoresis (PAGE).

Name	**Type**	**Sequence**	**Purification method**	**Purity***
let-7a	RNA	5-UGA GGU AGU AGG UUG UAU AGU U-3	HPLC	~92%
miR-15a	RNA	5-UAG CAG CAC AUA AUG GUU UGU G-3	HPLC	~90%
let-7a precursor	RNA	5-UGG GAU GAG GUA GUA GGU UGU AUA GUU UUA GGG UCA CAC CCA CCA CUG GGA GAU AAC UAU ACA AUC UAC UGU CUU UCC UA-3	PAGE	~40%
acr-7a	DNA	5-/Acr/ ATG AGG TAG TAG GTT GTA TAG TT-3	HPLC	~97%
acr-loop-pre7a	DNA	5-/Acr/ AAT CTC CCA GTG GTG GGT GTG ACC CTA A-3	HPLC	~96%
rep-7a	DNA	5-/Cy5/ AAA CTA TAC AAC CTA CTA CCT CA-3	PAGE	~99.9%

*Purity estimates based on estimates provided by suppliers (IDT/Genelink) or as measured with the Agilent Bioanalyzer 2100.

Table S2. Sourcemeter current program. We applied 1 μA constant current between ground (GND) and positive (HI) electrodes. A dash "-" under the reservoir listing indicates a floating voltage potential.

Name	**Duration (approx.)** [s]	**Laser power** [mW]	**Reservoir #**							
			1	**2**	**3**	**4**	**5**	**6**	**7**	**8**
Injection	410	1	GND	-	-	-	-	-	-	HI
Detection	190	1–4	-	-	-	-	-	GND	-	HI

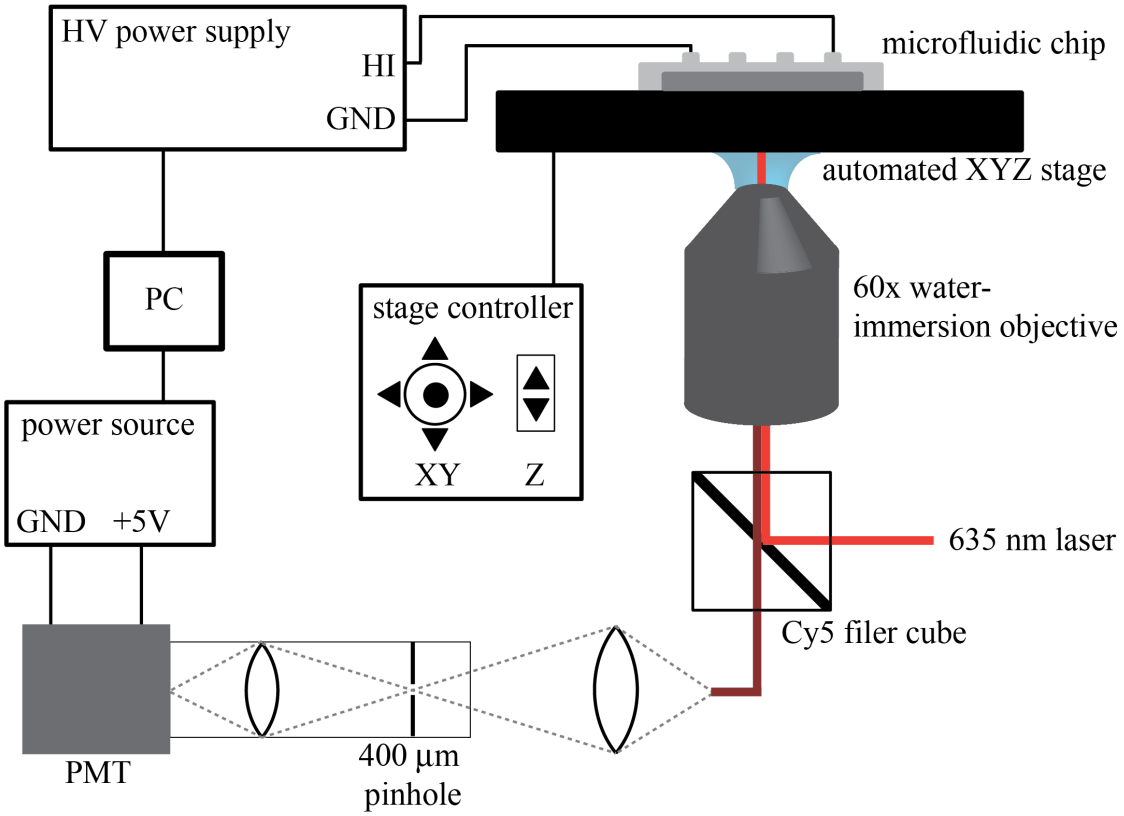

Figure S1. Schematic of experimental setup. We built a custom point-confocal setup around an inverted epifluorescent microscope which houses a high-numerical aperture objective and Cy5 filter cube. A custom optical train with a 400 µm pinhole attached to the microscope side port excludes out-of-plane light and re-focuses the captured light into the PMT module. We use a 635 nm diode laser connected to the microscope *via* a multimode fiber optic cable. We control the position of the microfluidic chip using an automated XYZ stage with controller. We use a high voltage sourcemeter to apply fixed current values to the microfluidic chip. Both the sourcemeter and PMT power supply are controlled and monitored by computer, using a custom MATLAB code.

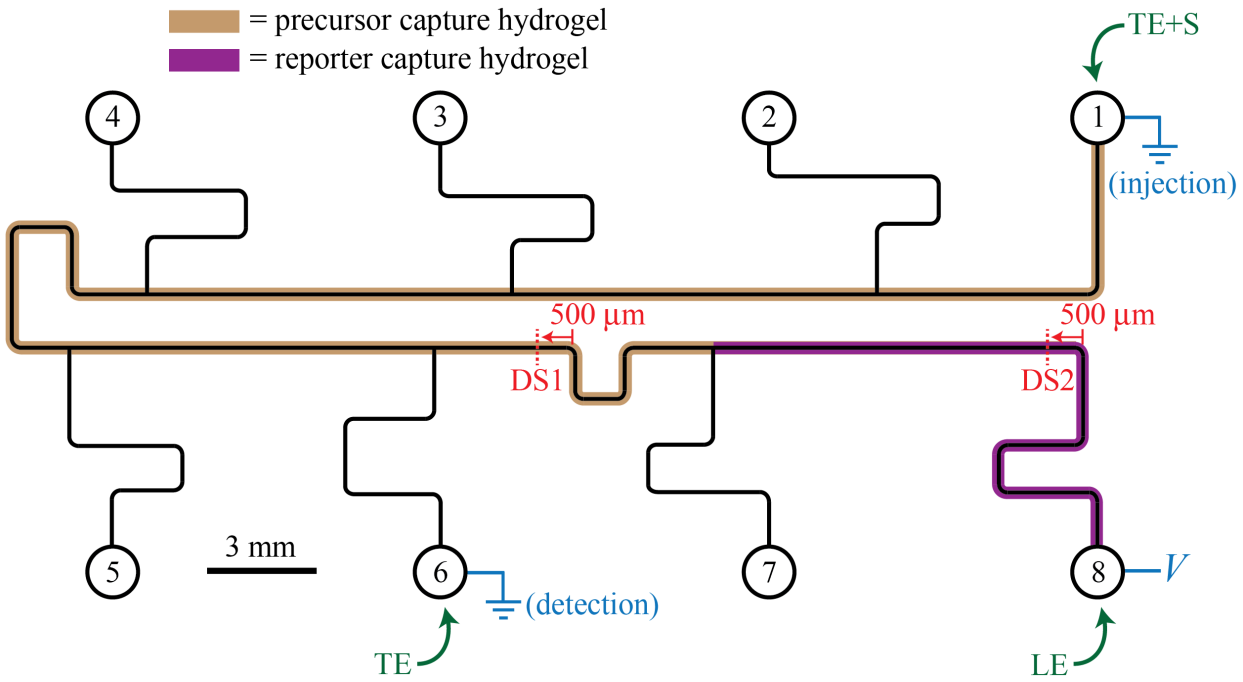

Figure S2. Caliper model NS260 microfluidic chip layout and indication of dispensed solutions (green), voltage program (blue), detection stations (red), and functionalized hydrogel layout (brown and purple). TE+S, TE, and LE were all dispensed prior to initiation of the voltage program. We applied the voltage program as described in **Section S6** and **Table S2**. We used detection station 1 (DS1) to monitor the peak location during injection. Once the peak passed DS1, we waited 5 s before turning off the voltage supply and switching the ground electrode from reservoir 1 to reservoir 6. We then commenced the detection voltage program and moved the detector to DS2.

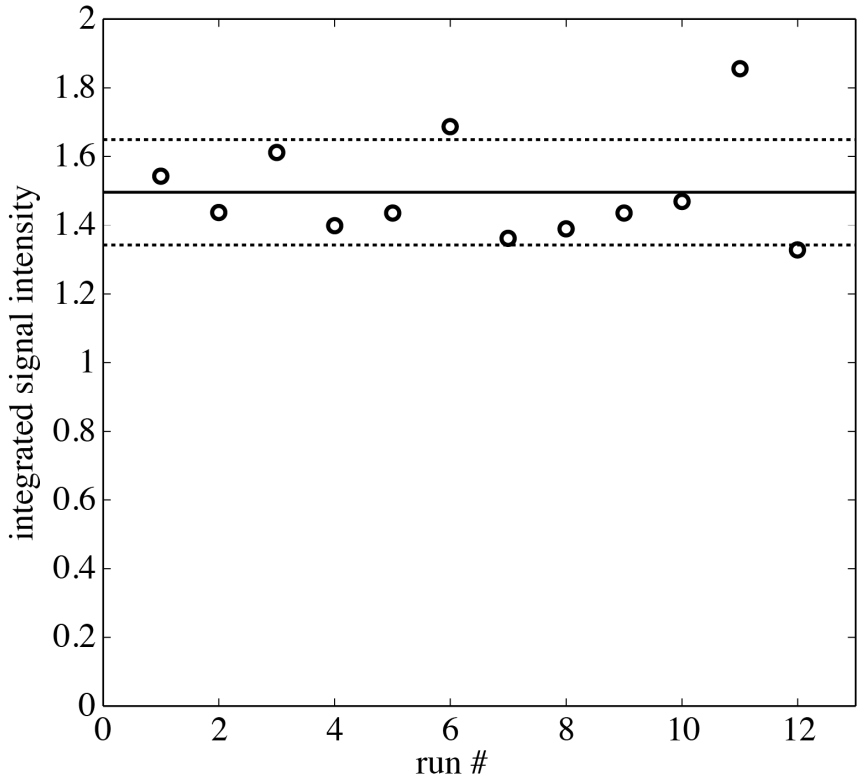

Figure S3. Integrated fluorescent intensity of injection peak for all experimental realizations demonstrating the limit of detection of 2.8 pM target concentration (includes three run each of the negative control, 2.8 pM and 140 pM let-7a, and 140 pM miR-15a). Symbols represent individual experiments. The solid black line represents the mean value and the dashed lines represent one standard deviation above and below the mean.

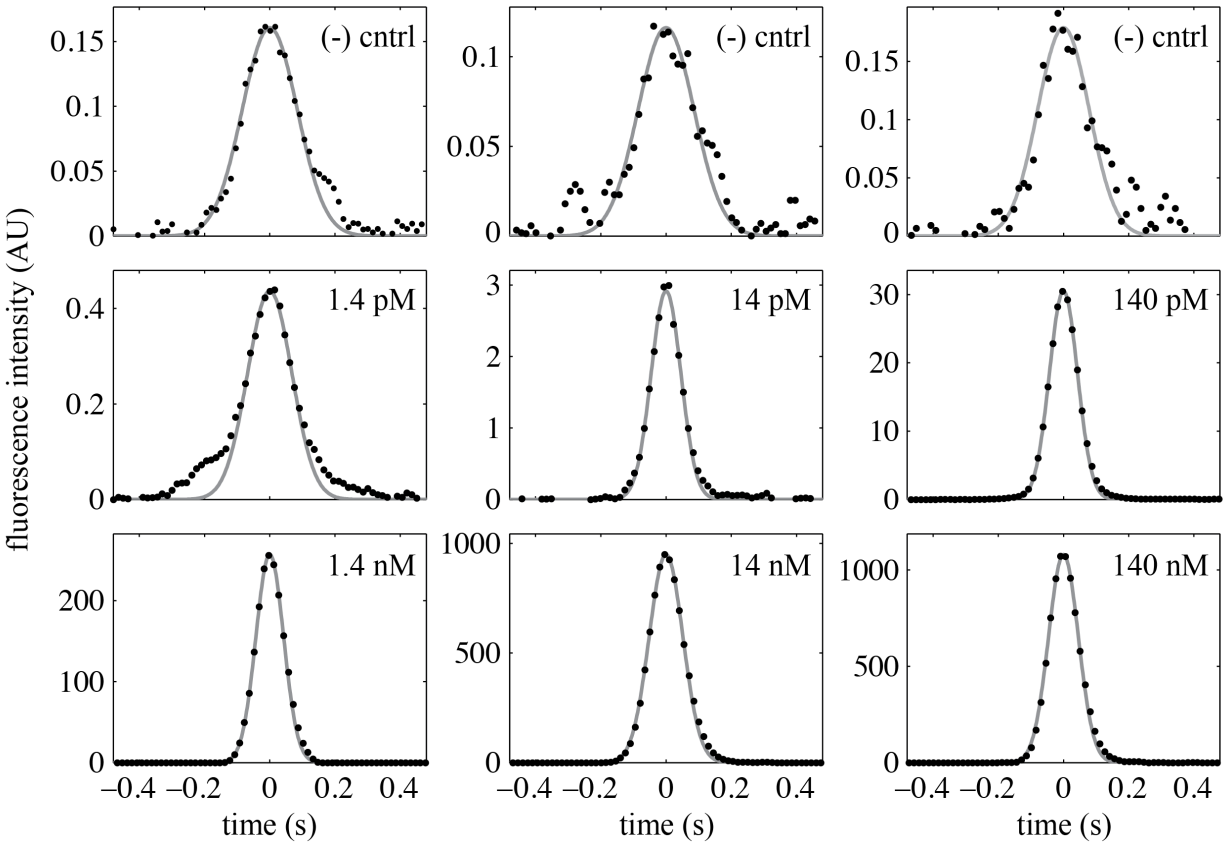

Figure S4. Raw, measured fluorescence intensity peaks together with Gaussian fits for our ITP gel capture assay. Each plot represents a different experiment with target concentration as given at the top right corner of the plot. For each case, we plot the signal measurement taken at location DS2 normalized by the integral of the corresponding injection peak measured at location DS1. Note the differences in the ordinance scales. We show experimental data as symbols and Gaussian fits as solid lines. We extend the fit down to a signal magnitude of 50% of the maximum intensity in the raw data.

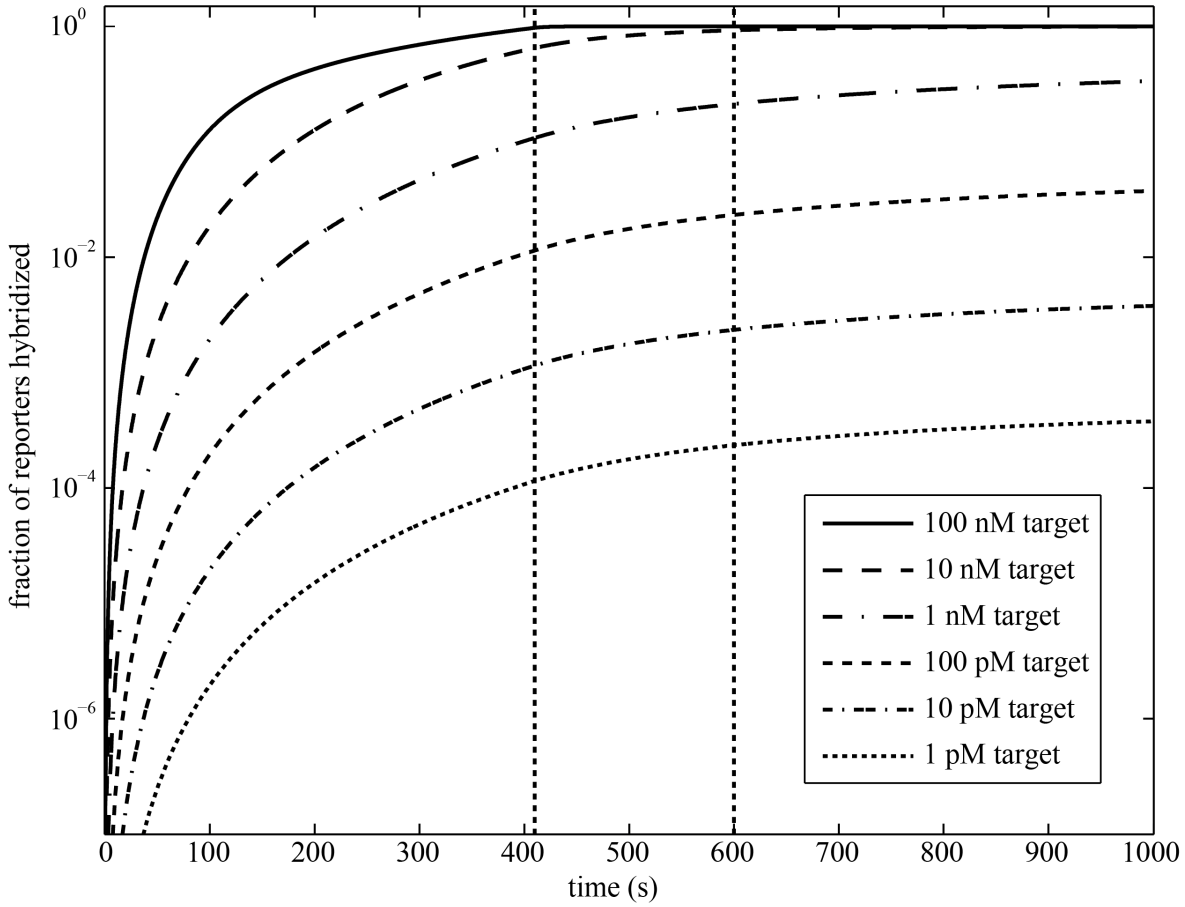

Figure S5. Predicted hybridization curves showing fraction of reporters hybridized *versus* time. The dashed vertical line at 410 s denotes the end of the sample injection. After this time, in the model, we set target and reporter flux into the ITP zone to zero ($F = 0$). The dashed vertical line at 600 s denotes the end of the detection portion of the assay.

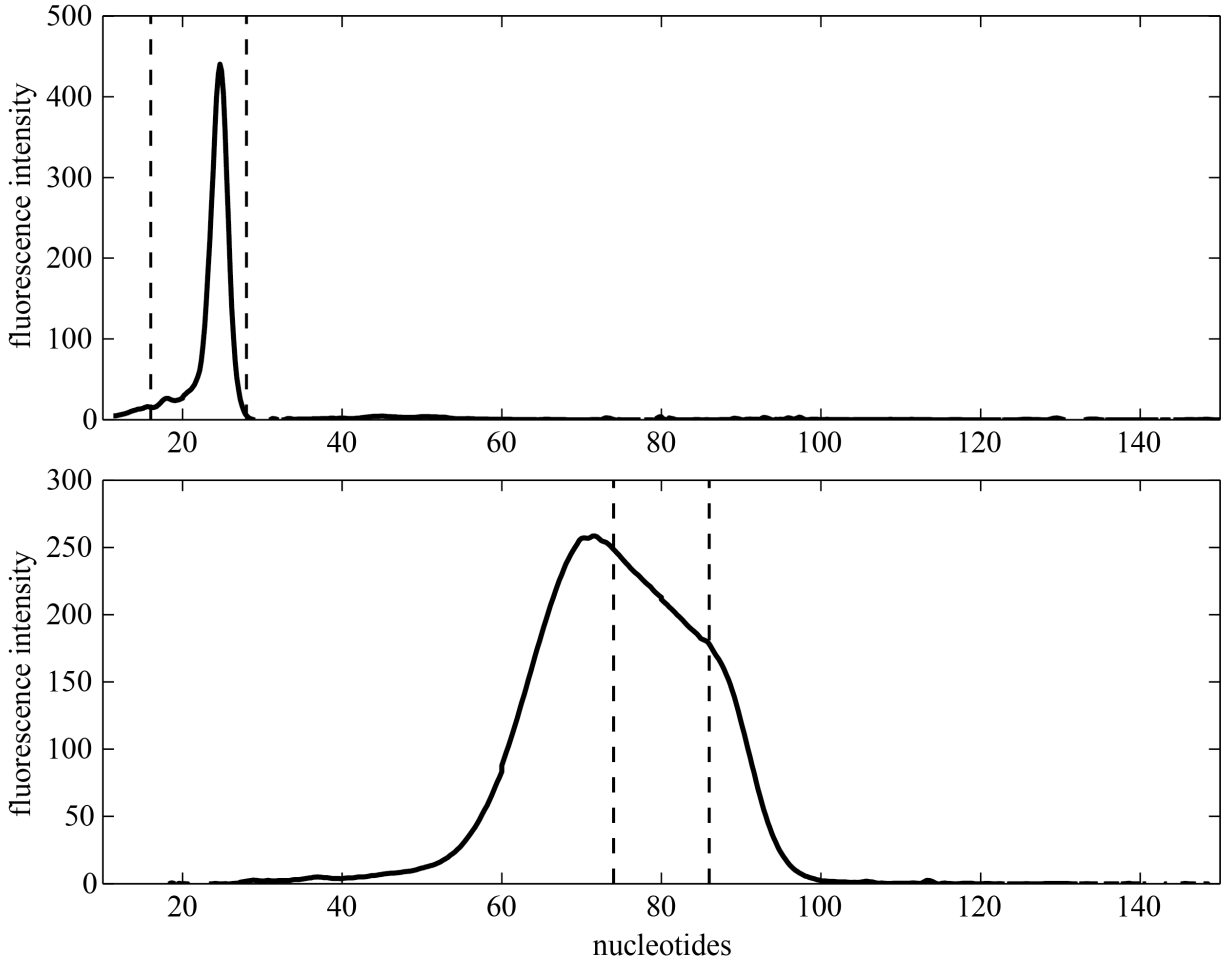

Figure S6. Electropherogram analyses (using Agilent Bioanalyzer 2100 electrophoresis instrument) of let-7a mature and precursor synthetic RNA oligos. Synthesized mature sequence of microRNA results in a sharp size distribution (top), suggesting high purity. However, difficulties in synthesizing longer RNA result in an electropherogram peak for the precursor sequence (bottom) which is much broader, suggesting much lower purity. The vertical dashed lines represent ±6 nt about the length of the correct oligo sequence (22 nt for mature, 80 nt for precursor). We estimate oligo purity by integrating this region and dividing by the overall electropherogram integral. Using this method, we estimate the mature oligo is ~92% pure, while the precursor oligo is only ~40% pure. We therefore attribute the high signal in experiments with pure precursor shown in **Fig. 3** to low purity of the precursor oligo. We hypothesize that the broad distribution contains a significant fraction of molecules containing the mature let-7a sequence, but lacking all or a significant portion of the critical loop sequence targeted by the immobilized probes in the functionalized gel designed for precursor removal.